What Use Are Crystal Field Parameters? A Chemist's Viewpoint

ARTICLE *in* THE JOURNAL OF PHYSICAL CHEMISTRY A · MAY 2010

Impact Factor: 2.69 · DOI: 10.1021/jp1015214 · Source: PubMed

2 AUTHORS:

Chang-Kui Duan
University of Science and Technology of C…
177 PUBLICATIONS **1,811** CITATIONS
SEE PROFILE

Peter Anthony Tanner
The Hong Kong Institute of Education
355 PUBLICATIONS **4,367** CITATIONS
SEE PROFILE

What Use Are Crystal Field Parameters? A Chemist's Viewpoint

Chang-Kui Duan and Peter A. Tanner*

Department of Biology and Chemistry, City University of Hong Kong, Tat Chee Avenue, Kowloon, Hong Kong S.A.R., P.R. China

Received: February 19, 2010; Revised Manuscript Received: March 31, 2010

Although first principles methods are gaining interest, the crystal field model is at present the only practicable model to analyze and simulate the energy level structures of lanthanide ions (Ln^{3+}) in crystal hosts at the accuracy level of $\sim$10 cm^{-1}. Three criteria are suggested to assess the use of energy parameters, especially crystal field parameters, from the crystal field parametrization of $4f^N$ energy level data sets for the entire lanthanide ion (Ln^{3+}) series, except Pm^{3+}. Systematic analyses have been performed upon the most complete energy level data sets available for Ln^{3+} situated at sites of high symmetry in crystals of $Cs_2NaLnCl_6$. This presents a stringent test for theory because the number of energy parameters is considerably reduced, and the data sets are representative and fairly complete. The results from these data set fittings are shown to comply with the three criteria put forward. First, the fittings of data sets are accurate, and a predictive capability has been employed to calculate the energy levels of Pm^{3+} and to elucidate and list all of the potentially luminescent levels of Ln^{3+} in the hexachloroelpasolite hosts. Second, the systematic and smooth variations of parameter values over the lanthanide series have been described by simple equations and rationalized. Third, a physical insight of the crystal field parameter variation across this series of elements has been achieved by utilizing a simple semiquantitative model considering the distributions of the 4f radial wave functions at the edge of the Ln^{3+} ions, where the ligand orbitals extend. The parameter trends for an individual Ln^{3+} ion have been shown to be consistent also for the Cs_2NaLnF_6 host lattice, and predictions of the individual crystal field parameter values are made.

Introduction

Although first principles methods are of current interest, the crystal field model is at present the only practicable model to analyze and simulate the energy level data sets of lanthanide ions (Ln^{3+}) in crystal hosts at the accuracy level of $\sim$10 cm^{-1}. A Scopus search of "crystal field" shows more than 14 000 hits, whereas there are 2131 hits for "crystal field parameters". This study recognizes that in order to be useful, certain criteria should be fulfilled by these parameters, which are the outcome of the fitting procedure.

First, not only should the energy level fitting accurately reproduce the experimental data set, but it should also predict missing or unexplored energy levels. It is a prerequisite that the energy level data set is representative (i.e., extending over a wide range) and fairly complete. Although not considered in detail in the present study, it is noted that the wave functions resulting from the parametrization should be capable of accurately predicting other properties such as g-factors and spectral intensities.

Second, the parameters are expected to show some type of systematic variation for materials comprising a series of closely related elements.

Third, the parameters should be related to other physical quantities in a systematic manner. Also the parameters should show explicable trends over various crystal hosts for a particular ion.

We cannot observe that these criteria have been fulfilled for studies of energy levels of the $4f^N$ configuration of lanthanide ions (Ln^{3+}) in previous studies. Energy level parametrizations of some systems (e.g., Ln^{3+} doped in $Y_3Al_5O_{12}$,[1] $LiYF_4$,[2] YPO_4,[3] LaX_3 (X = Cl, F),[4] LnOCl,[5]) have employed large data sets, and the energy fitting of observed levels has resulted in a standard deviation even less than 10 cm^{-1}. However, since Ln^{3+} in these systems are situated at sites of relatively low symmetry, many fitting parameters were required. Methods for reducing the number of parameters were to employ fixed ratios for certain parameter subsets, or to adopt a pseudosite symmetry for Ln^{3+}, such as D_{3h} for the C_2 site of Ln^{3+} in LaF_3. However, often, the uncertainty or error in one parameter forces other parameters into incorrect values. Furthermore, various different potential minima may exist for a set of many parameters. Hence, the second criterion above has not been well-satisfied for the mentioned systems, and the parameter variations that have been produced from these data set fittings are rather irregular over the entire Ln^{3+} series. In other cases, the data sets have not been numerically adequate to accurately fix parameter values, or due to some inaccurate energy values included in the data set the fitted parameter values are unrealistic. Some previous presentations of parameter values for the entire lanthanide series have been given for Ln^{3+} doped in LaF_3 and $LaCl_3$.[4]

The electronic spectra of Ln^{3+} in hexachloroelpasolite systems have received much attention, and previous studies were reviewed in 2004.[6] The electronic spectra have been extensively interpreted and employed to elucidate the $4f^N$ energy levels of Ln^{3+} in this host. The major advantage of this type of crystal lattice is that the octahedrally coordinated Ln^{3+} are situated at sites of O_h symmetry. Therefore, only two crystal field parameters are required for the analysis of the energy level data set, which presents a stringent test for theory. The crystal field energy levels are labeled by irreducible representations of the group O for even N, or the double group O' for odd N, where

* To whom correspondence should be addressed. E-mail: bhtan@cityu.edu.hk.

10.1021/jp1015214
Published on Web 04/22/2010

the parity (not shown) is g or u, respectively. Previous crystal field analyses employed rather sparse energy level data sets,[7] and there were errors in some matrix elements.[8] However, new experimental studies using luminescence, absorption, and two-photon spectroscopy have produced more extensive data sets upon which our analyses are based.[9]

The present study shows that the above three criteria can now be satisfied by lanthanide ions (Ln^{3+}) in these elpasolite host lattices, $Cs_2NaLnCl_6$.

Theoretical Calculations. A brief summary of the $4f^N$ energy level parametrization method for lanthanide ions is now given, and the description of the parameters follows Carnall et al.[4] and Crosswhite and Crosswhite.[10] The energy levels, E_i, of the $4f^N$ configuration of lanthanide ions in a crystal can be analyzed with a parametric model employing an effective-operator Hamiltonian, H, expressed as a matrix that is diagonalized to give also the corresponding wave functions, Ψ_i:

$$(H - E_i)\Psi_i = 0 \tag{1}$$

where

$$H = H_{AT} + H_{CF} + H_{ADD} \tag{2}$$

where H_{AT} comprises the pseudofree ion or atomic Hamiltonian, including all interactions that are spherically symmetric; H_{CF} is the operator comprising the nonspherically symmetric crystal field; and H_{ADD} contains other interactions. The atomic Hamiltonian is expressed:

$$\begin{aligned} H_{AT} = E_{AV} + \sum_k F^k \mathbf{f}_k + \sum_i \zeta_f \mathbf{s}_i \cdot \mathbf{l}_i + \\ \alpha L(L+1) + \beta G(G_2) + \gamma G(R_7) \\ + \sum_s T^s \mathbf{t}_s + \sum_k P^k \mathbf{p}_k + \sum_j M^j \mathbf{m}_j \end{aligned} \tag{3}$$

where $s = 2, 3, 4, 6, 7, 8$; $k = 2, 4, 6$; and $j = 0, 2, 4$. The first term E_{AV} (containing F^0) adjusts the configuration barycenter energy with respect to other configurations. The Slater parameters F^k represent the electron−electron repulsion interactions and are two-electron radial integrals, where the $\mathbf{f}_k$ represent the angular operator parts of the interactions. These two parameters are the most important in determining the atomic energies. The electrostatic parameters F^k largely determine the multiplet ^{2S+1}L barycenters whereas the spin−orbit coupling parameter determines the splitting of each multiplet $^{2S+1}L_J$. The two-body configuration interaction parameters α, β, γ, parametrize the second-order Coulomb interactions with higher configurations of the same parity. The operators $G(G_2)$ and $G(R_7)$ are Casimir's operators for the groups G_2 and R_7, and $L(L+1)$ is the eigenvalue of the square of the angular momentum operator, $\mathbf{L}^2$. Changes in these parameters cause shifts of up to a few hundreds of cm^{-1} for energy levels. For $4f^N$ and $4f^{14-N}$, $N > 2$ the three body parameters T^s are employed to represent Coulomb interactions with configurations that differ in the quantum numbers of a single electron from $4f^N$. With the inclusion of these parameters, the free ion energy levels can usually be fitted to within 100 cm^{-1}. Smaller corrections to energy levels arise from magnetically correlated interactions. The Marvin integrals M^j describe the spin−spin and spin-other orbit relativistic interactions between electrons, and the P^k represent two-body magnetic interactions, of which the most important is the electrostatically correlated spin−orbit perturbation involving the excitation of a 4f electron into a higher-lying f orbital. Usually the ratios $M^0:M^2:M^4$ and those of $P^2:P^4:P^6$ are constrained to minimize the number of parameters, which otherwise already total 20. To be consistent, we have utilized the same ratios for all Ln^{3+}.

The splitting of J levels of Ln^{3+} in the crystal, and the J-mixing between different multiplets by crystal field levels belonging to the same symmetry irreducible representation is determined by the nonspherically symmetric components of the one-electron crystal field interactions, where the crystal field Hamiltonian is given by:

$$\begin{aligned} H_{CF} = \sum_{i=1}^{N} \sum_{k=0}^{\infty} [B_0^k C_0^k(i) + \sum_{q=1}^{k} (B_q^k (C_{-q}^k(i) + (-1)^q C_q^k(i)) + \\ B_q'^k i (C_{-q}^k(i) - (-1)^q C_q^k(i)))] \end{aligned} \tag{4}$$

The spherical tensor $C_q^k(i)$ of rank k depends upon the coordinates of the ith electron and the summation is over all 4f electrons of the Ln^{3+} ion. The nonzero crystal field parameters for the O_h point group reduce to B_0^4, B_4^4, B_0^6, and B_4^6, and since $B_4^4 = \sqrt{(5/14)}B_0^4$ and $B_4^6 = -\sqrt{(7/2)}B_0^6$, only two additional parameters are required to model the splittings of J terms by the octahedral crystal field. For low symmetry systems up to 27 crystal field parameters may be required for analysis. Note that the Wybourne spherical tensorial notation is adopted herein, and in the cubic environment, the relationship with unit tensor normalized crystal field parameters is $B_0^{(4)} = 1.128B_0^4$, and $B_0^{(6)} = -1.277B_0^6$. In the following and in Tables, B_0^4 and B_0^6 are abbreviated as B_4 and B_6, respectively, and refer to Ln^{3+} in $Cs_2NaLnCl_6$ unless otherwise stated.

Results and Discussion

The energy level data sets for the entire Ln^{3+} series in $Cs_2NaLnCl_6$ have been systematically analyzed and parametrized by eqs 1−4 in this study. A summary of the derived parameters and the characteristics of the data sets are included in Table 1. The number of parameters employed (N_p) to fit each Ln^{3+} crystal field energy level data set of N_{expt} experimentally determined levels (out of a possible total number N_{el}, corresponding to N_{st} nondegenerate states) is given in each case, together with the standard deviation of the fit, σ. Note that the analyses of the small $4f^1$ and $4f^{13}$ data sets (comprising only 5 crystal field levels) only require spin−orbit and crystal field parameters, together with the parameter E_{AV}, so that $N_p = 4$. The representivity ($100 \times N_{exp}/N_{el}$) of the data set does vary considerably for different Ln^{3+}, being 100% for Ce^{3+}, Yb^{3+}; over 90% for Pr^{3+}, Tm^{3+}, but much less for the more extensive $4f^N$ configurations, such as 3% for Gd^{3+}. The standard deviations of most fits are around 20 cm^{-1}. Whereas the experimental errors in determining crystal field splittings within a given multiplet term are generally small (several cm^{-1}), the calibration errors for higher energy levels are considerably higher, as shown by the systematic errors of 10−20 cm^{-1} between different experimental studies. Notably, the standard deviations of the energy levels in the fits for Pr^{3+}, Nd^{3+}, and Tm^{3+} are higher. It has been demonstrated[9] that additional terms (H_{ADD}) explicitly involving configuration interaction are required to fit certain multiplets in these cases. In order to present a uniform fitting methodology for the comparison of the energy levels of different Ln^{3+} systems, these additional terms have been omitted. In some other cases (Yb^{3+}, Gd^{3+}), the standard deviations of certain parameters are very large. For Gd^{3+} this may result from the sparse energy

TABLE 1: Parameters for the Calculated $4f^N$ Energy Levels of Ln^{3+} in $Cs_2NaLnCl_6$[a]

Ln^{3+}	Ce		Pr		Nd		Pm	Sm		Eu		Gd		Tb		Dy		Ho		Er		Tm		Yb	
Z	58		59		60		61	62		63		64		65		66		67		68		69		70	
N	1		2		3		4	5		6		7		8		9		10		11		12		13	
E_{AVG}	1667.1	0.7	10 184	7	23 991	13	36 331	47 072	35	62 676	31	87 281	26	68 007	85	55 813	168	48 025	21	35 325	6	17 808	8	4610	15
ζ_{4f}	623.2	0.4	744	4	874	5	999	1164	2	1331	2	1503	4	1697	3	1896	14	2101	5	2363	2	2613	3	2894	9
B_4	2119.5	4.3	2059	62	1971	51	1958	1832	33	1936	23	1839	99	1686	28	1652	46	1643	47	1531	56	1491	54	1422	89
B_6	260.7	5.6	237	35	249	31	24	274	20	245	16	112	127	228	18	178	25	151	22	160	20	152	29	86	106
F^2			67 776	69	71 215	188	74 254	78 016	202	79 688	109	85 433	98	88 435	389	91 010	597	92 614	147	96 736	59	100 303	128		
F^4			49 846	229	51 784	371	54 086	56 354	367	61 547	229	59 484	72	63 031	554	64 550	1285	66 981	579	68 455	114	70 385	251		
F^6			32 787	179	35 025	171	38 388	39 737	206	43 044	131	44 653	37	45 027	433	50 167	1126	49 666	277	51 008	112	50 286	366		
α			23.3	0.6	21.5	0.4	14.5	21.3	0.5	27.7	0.5	18.0		19.0	0.9	17.8	3.4	22.08	1.2	17.4	0.4	18.0			
β			−644		−650	23	−646	−710	20	−1272	47	−620		−568	36	−597	157	−714	30	−658	19	−645			
γ			1413		1616	58	1509	1699	97	1461	47	1658		1754	154	1352	231	2046	95	1900		2134			
M^0			1.88		1.47	0.52	2.19	2.48	0.23	2.13	0.08	3.17	0.06	4.26	0.29	3.66	1.23	3.04	0.44	3.94	0.25	4.06	0.68		
P^2			244		135	97	283	359	51	195		542		851	89	568	183	118	100	510					
T^2					336	65	306	246	15	278	8	308		105	40	311		365		120					
T^3					42	7	45	25	11	40		43		40		12		37		52	9				
T^4					65	10	34	18	34	40		51		45		12		95		27	10				
T^6					−275	20	−314	−158	54	−546	83	−298		−365		−474		−274		−296	31				
T^7					342	39	557	253	21	244	23	338		320		413		331		195	31				
T^8					290	47	407	379	15	241	18	335		139	46	315		343		176					
σ	0		38.5		32.9			17.2		15.3		12.2		21.8		15.8		19.1		22.1		30.1		31.6	
δ	0		33.9		29.2			15.4		14.2		10.8		20.6		13.0		17.4		19.3		26.0		14.1	
N_{st}	14		91		364		1001	2002		3003		3432		3003		2002		1001		364		91		14	
N_{el}	5		40		120		421	666		1261		1146		1262		666		421		120		37		5	
N_p	4		8		18		0	18		11		8		14		12		12		14		8		4	
N_{expt}	5		36		86		0	91		77		36		130		37		69		59		31		5	

[a] Energy level parameters (from E_{AV} to T^8), the standard deviation of the optimization (σ), and the mean deviation (δ) are in units of cm^{-1}; N, N_{st}, N_{el}, N_p, and N_{expt} are numbers of 4f electrons, states of $4f^N$, energy levels of $4f^N$, parameters, and measured energy levels, respectively. For each ion, the first column contains the best fitted values or fixed values used in energy level calculation. The second column contains the uncertainties for the fitted parameters (blanks mean the corresponding parameter is fixed rather than fitted). The parameters for Pm are obtained by interpolations (from ζ_{4f} to P^2) or adopting the quasi-free-ion value.

TABLE 2: Predicted $4f^N$ Luminescent Levels (Using the Energy Gap Law $E_{gap} > 4\ E_{phonon} \sim 1200\ cm^{-1}$) with Energies up to 57 000 cm^{-1} [a]

Ln^{3+}	$^{2S+1}L_J$	IR	E_{calc}	E_{expt}	E_{gap}	lum	Ln^{3+}	$^{2S+1}L_J$	IR	E_{calc}	E_{expt}	E_{gap}	lum
Ce	$^2F_{7/2}$	E″	2160	2160	1590	?	Tb	$^5D_3$	A_2	26 200	26 219	5612	√
Pr	$^3H_5$	T_1	2280	2300	1614	?	Tb	$^5H_6$	A_1	32 785	32 732	1333	?
Pr	$^3H_6$	E	4376	4386	1678	?	Dy	$^6H_{13}$	U	3587	3606	3185	?
Pr	$^3F_3$	*T_2	6583	6616	1330	?	Dy	$^6H_{11/2}$	E′	5917	5929	2191	?
Pr	$^1G_4$	A_1	9728	9847	2484	√	Dy	$^6H_{9/2}$	U	7692	7713	1661	?
Pr	$^1D_2$	T_2	16 661	16 666	6235	√	Dy	$^6F_{5/2}$	E″	12 396	12 392	1302	√
Pr	$^3P_0$	A_1	20 604	20 625	3418	√	Dy	$^4F_{9/2}$	U	20 964	20 957	7182	√
Pr	$^1S_0$	A_1	46 380		23 967	×	Dy	$^4F_{5/2}$	E″	40 051		1233	?
Nd	$^4I_{11/2}$	U	1893	1921	1562	?	Ho	$^5I_7$	T_1	5088	5116	4805	√
Nd	$^4I_{13/2}$	E″	3828	3861	1695	?	Ho	$^5I_6$	E	8602	8620	3346	√
Nd	$^4I_{15/2}$	U	5771	5797	1664	?	Ho	$^5I_5$	T_1	11 183	11 198	2434	√
Nd	$^4F_{3/2}$	U	11 309	11 335	5129	√	Ho	$^5I_4$	A_1	13 225	13 232	1939	√
Nd	$^4G_{7/2}$	E″	18 620	18 640	1377	√	Ho	$^5F_5$	T_1	15 317	15 353	1869	√
Nd	$^2P_{1/2}$	E′	23 005	23 043	1289	?	Ho	$^5S_2$	T_2	18 370	18 365	2809	√
Nd	$^2P_{3/2}$	U	25 933		2300	?	Ho	$^5F_3$	A_2	20 384	20 420	1849	√
Nd	$^4D_{3/2}$	U	27 602	27 617	1669	√	Ho	$^5G_5$	T_1	23 794	23 779	1529	?
Nd	$^2F_{5/2}$	U	37 898	37 838	3866	?	Ho	$^5G_4$	A_1	25 673	25 719	1745	√
Nd	$^2F_{7/2}$	E′	39 253		1257	?	Ho	$^3D_3$	T_1	32 928		2129	?
Nd	$^2G_{9/2}$	U	46 884		7495	?	Ho	$^5D_4$	A_1	41 166	41 163	1228	√
Pm	$^5I_5$	T_1	1578		1321	?	Ho	$^1D_2$	T_2	44 749		1913	?
Pm	$^5I_6$	A_1	3151		1445	?	Er	$^4I_{13/2}$	E′	6490	6492	6188	√
Pm	$^5I_7$	T_1	4804		1523	?	Er	$^4I_{11/2}$	E′	10 165	10 166	3469	√
Pm	$^5I_8$	E	6480		1491	?	Er	$^4I_{9/2}$	U	12 344	12 357	2079	√
Pm	$^5F_1$	T_1	12 241		5401	?	Er	$^4F_{9/2}$	U	15 172	15 152	2651	√
Pm	$^3K_8$	E	19 603		1408	?	Er	$^4S_{3/2}$	U	18 272	18 265	2923	√
Pm	$^3G_3$	A_2	21 440		1260	?	Er	$^4F_{7/2}$	E′	20 388	20 374	1238	√
Pm	$^3F_4$	A_1	35 230		1541	?	Er	$^4F_{5/2}$	U	22 079	22 056	1622	?
Pm	$^3G_5$	T_2	41 592		1224	?	Er	$^4F_{9/2}$	U	24 369	24 425	1926	√
Pm	$^1G_4$	T_2	46 895		1565	?	Er	$^4G_{11/2}$	U	26 131	26 098	1613	√
Pm	$^1L_8$	T_2	49 215		1688	?	Er	$^2P_{3/2}$	U	31 369	31 367	3387	?
Pm	$^1I_6$	A_2	55 016		1590	?	Er	$^2K_{13/2}$	E′	32 613	32 613	1244	√
Pm	$^1G_4$	A_1	56 607		1235	?	Er	$^2H_{9/2}$	U	36 252	36 224	1598	√
Sm	$^6H_{13/2}$	U	5028	5005	1310	?	Er	$^4D_{5/2}$	E″	38 168	38 164	1799	?
Sm	$^6F_{11/2}$	E′	10 458	10 461	1254	?	Er	$^2I_{11/2}$	E″	40 674	40 668	1720	√
Sm	$^4G_{5/2}$	U	17 747	17 742	7120	√	Er	$^4D_{1/2}$	E′	46 600		3191	?
Eu	$^5D_0$	A_1	17 209	17 208	11 938	√	Er	$^2H_{11/2}$	U	50 514		1935	?
Eu	$^5D_1$	T_1	18 961	18 961	1752	√	Er	$^2F_{7/2}$	E′	53 846		2964	?
Eu	$^5D_2$	T_2	21 393	21 385	2432	√	Tm	$^3F_4$	T_2	5577	5547	5103	√
Eu	$^5D_3$	T_1	24 281	24 261	2810	√	Tm	$^3H_5$	T_1	8275	8240	2293	√
Eu	$^5H_3$	T_1	30 563		1839	?	Tm	$^3H_4$	T_2	12 572	12 538	3968	√
Gd	$^6P_{7/2}$	E″	31 940	31 954	31 940	√	Tm	$^3F_3$	*A_2	14 381	14 428	1445	√
Gd	$^6I_{7/2}$	E″	35 624	35 623	2485	√	Tm	$^1G_4$	T_2	20 952	20 852	5799	√
Gd	$^6D_{9/2}$	E′	39 233	39 219	2736	?	Tm	$^1D_2$	T_2	27 697	27 653	6171	√
Gd	$^6G_{7/2}$	E″	48 957		8226	?	Tm	$^1I_6$	E	34 332	34 117	6579	√
Tb	$^7F_5$	T_1	2071	2083	1703	?	Tm	$^3P_2$	E	37 543	37 462	1609	√
Tb	$^5D_4$	A_1	20 457	20 470	14 620	√	Yb	$^2F_{5/2}$	U	10 276	10 248	9680	√

[a] Here E_{calc}, E_{expt}, E_{gap}, $^{2S+1}L_J$, and IR are the calculated energy, experimental energy, calculated energy gap below the level, the multiplet term, and the irreducible representation, respectively, of the predicted luminescent level. The column lum depicts whether luminescence has been experimentally observed (√), whether luminescence does not occur (×), or if the investigation has not been made conclusively (?). The energy units are cm^{-1}. Refer to the text for discussion, including the starred items in column IR.

level data set, whereas for Yb^{3+} the fitting is rather insensitive to variation of the crystal field parameters.

Now the various criteria mentioned above are evaluated for the results of our energy parametrizations. Two remarks are made considering the first criterion concerning prediction. First, by interpolation, parameter values for Ln = Pm are listed in Table 1. These parameters have been employed to calculate the $4f^4$ energy levels of Pm^{3+} in $Cs_2NaPmCl_6$, up to the band gap estimated at ~7.5 eV (~60 500 cm^{-1}).[11] These levels are listed in the Supporting Information (Table S1). Second, in the absence of concentration quenching and cross-relaxation phenomena, it is established that luminescence occurs from a suitably populated crystal field level provided that it is separated from the next-lower level by more than four phonons.[12] For the $Cs_2NaLnCl_6$ series the highest energy phonon is the Ln−Cl totally symmetric stretching vibration, between 279 cm^{-1} (Ln = Ce) and 296 cm^{-1} (Ln = Yb).[6] Therefore, we take as the rough criterion that luminescence will occur provided the energy gap is >1200 cm^{-1}. Table 2 lists the predicted $4f^N$ luminescent levels of the lanthanide ions doped in hexachloroelpasolite host lattices, up to the average band gap of 57 000 cm^{-1}. For a given Ln^{3+} energy level, when the excitation energy is greater than the energy required to ionize an electron from the ion into the conduction band of the host lattice, photoionization occurs. The identifications are included for levels from which luminescence has been experimentally observed (by ticks), conclusively not observed (by crosses), or not conclusively investigated (by question marks). Experiments have demonstrated that there are some other multiplet terms that are luminescent at room temperature due to thermal population (such as $^3P_1$ for Pr^{3+}; $^4F_{5/2}$ for Nd^{3+}; $^5F_4$ for Ho^{3+}; and $^2H_{11/2}$ for Er^{3+}) but these are not included. Some of the question marks refer to levels either where

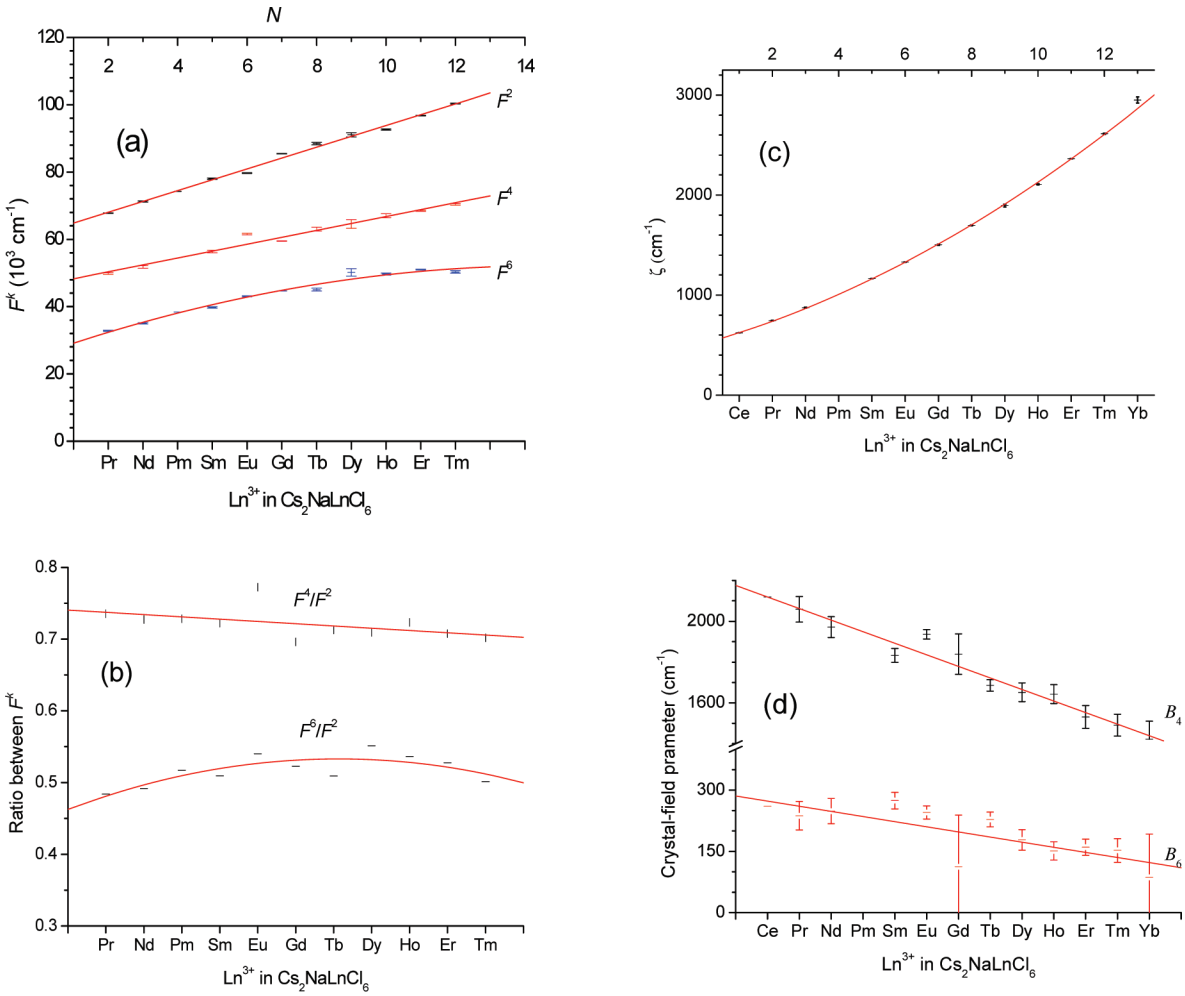

Figure 1. Variation of the energy parameters from fittings of Ln^{3+} energy data sets of $Cs_2NaLnCl_6$. N is the number of electrons in the configuration $4f^N$. (a) Coulomb parameters F^k; (b) ratios of Coulomb parameters; (c) spin−orbit interaction, ζ_{4f}; (d) crystal field parameters B_4 and B_6.

appropriate excitation has not been employed, or where cross-relaxation processes cause deactivation in concentrated materials and suitable dilution into a transparent hexachloroelpasolite host has not yet been performed. There are certainly many more potentially luminescent levels of hexachloroelpasolites to be investigated. However, to our knowledge, no other luminescent levels for these systems have previously been reported, verifying good prediction of the calculations. Some interesting potential luminescent candidates are Ce^{3+} and Sm^{3+} for infrared emission, whereas the failure of Sm^{3+} to emit above 17 735 cm^{-1} is notable. The only nonluminescent level (with a cross) in Table 2 is Pr^{3+} $^1S_0$, which is situated above the lowest 4f5d level located at 39 017 cm^{-1} so that nonradiative deactivation occurs to this configuration. In two cases (starred in the Table) the predicted irreducible representation of the emitting level does not agree with experiment (T_1 for Pr^{3+}; T_1 for Tm^{3+}) since the relevant energy levels are fairly close together, and the determined lowest energy is listed.

Also mentioned in the first criterion is the ability to predict spectral intensities using the wave functions generated in the parametrization. This topic is too extensive and complex to discuss herein, but a brief note is made. This type of prediction will be particularly difficult for transitions that are essentially forbidden, but which can gain intensity by minute mixing of a state wave function for which the transition is allowed. We have recently fitted the two-photon absorption spectrum of $Cs_2NaGdCl_6$ utilizing the wave functions from the fitting of the rather sparse Gd^{3+} data set. The agreement with experiment over a wide range of intensities is good.[13]

The second criterion above refers to systematic variation. The results from Table 1 enable comparisons to be made of the energy parameters across the entire lanthanide series. Figure 1a shows the variation of the Slater parameters F^k, and there is an overall increase across the series. The best fits using a linear relation or a second-order polynomial are (in units of cm^{-1}):

$$F^2 = (61573 \pm 610) + (3223.3 \pm 79.4)N \quad (5)$$

$$F^4 = (46213 \pm 830) + (2054 \pm 108)N \quad (6)$$

$$F^6 = (25631 \pm 1620) + (3594.3 \pm 18)N - (121.6 \pm 36.4)N^2 \quad (7)$$

In the central field approximation,[14] a Coulomb field is characterized by the effective nuclear charge, with the ratios F^4/F^2 and F^6/F^2 being stable for Ln^{3+}, at 0.70 and 0.54, respectively. These ratios are nearly satisfied for Ln^{3+} in the midseries, but the individual trends for these ratios are different (Figure 1b).

$$F^4/F^2 = (0.7437 \pm 0.0138) - (0.00316 \pm 0.00180)N \quad (8)$$

$$F^6/F^2 = 0.4413 + (0.02261 \pm 0.0069)N - (0.0014 \pm 0.00048)N^2 \quad (9)$$

The comparison with the free-ion values of these parameters may be made, for example, with the data for Pr^{3+},[15] where the magnitudes of F^k are 7.5 ± 1.2% smaller in the $Cs_2NaPrCl_6$ crystal. This nephelauxetic effect has been ascribed to various causes, including the reduced repulsion between f electrons due to interpenetration of ligand electrons.

The spin orbit coupling parameter shows a smooth variation across the Ln^{3+} series (Figure 1c). The best fit with a second-order polynomial is (in units of cm^{-1}):

$$\zeta_{4f} = (539.4 \pm 10.2) + (87.82 \pm 3.33)N + (7.095 \pm 0.233)N^2 \quad (10)$$

The variations of the energy of the $4f^N$ configuration barycenter relative to the ground state of the configuration, the two-body configuration interaction parameters and the M^j, P^k, and T^s parameters are shown in the Supporting Information (Figures S1−S3) and show systematic trends.

The reported trends for the crystal field parameters B_4 and B_6 from previous experimental studies have not been smooth (as shown, for example, in ref 7), but the plots in Figure 1d can be fitted by linear relations (in units of cm^{-1}):

$$B_4 = (2176.2 \pm 29.2) - (56.7 \pm 3.6)N \quad (11)$$

$$B_6 = (285.5 \pm 24.6) - (12.6 \pm 3.0)N \quad (12)$$

The ratio B_6/B_4 across the series of Ln^{3+} in $Cs_2NaLnCl_6$ fluctuates considerably but is subject to large errors in some cases (Figure S4). The ratio shows a slight decrease across the series and can be fitted versus N in a linear relation as shown in the figure, within the uncertainties of the ratio.

The crystal-field parameters for the point charge model vary according to $r^k/[R(\text{Ln}-\text{Cl})]^{(k+1)}$, where r^k ($k = 4, 6$) are the radial integrals $\langle 4f|r^4|4f\rangle$ and $\langle 4f|r^6|4f\rangle$, respectively and R(Ln−Cl) is the metal−ligand distance. This model therefore predicts that the ratio $B_4(Yb^{3+})/B_4(Ce^{3+}) \sim 0.35$ and $B_6(Yb^{3+})/B_6(Ce^{3+}) \sim 0.24$, which are far from the optimized crystal-field parameter ratios of 0.67 and 0.33 herein. This indicates that main contribution to crystal-field interaction may not be the point charge of the ligands. Faulkner et al.[16] calculated the trends in the crystal field parameters B_4 and B_6 across the lanthanide series for $Cs_2NaLnCl_6$. The model employed by these authors included two types of Ln^{3+}-ion interaction: multipole (Ln^{3+})-point charge and charge (Ln^{3+})-induced dipole, with the latter making the dominant contributions to the both crystal field coefficients. Notably, the six chloride ions in the first coordination sphere, $LnCl_6^{3-}$, were found to contribute >95% of the B_4 and B_6 values. The calculated B_4 values are in reasonable agreement with those from the present study, whereas the B_6 values are several times too small. However, the trends for both calculated parameters from ref 16 can be fitted best by second-order polynominals, presumably with the radial integrals playing a dominant role. This result differs from the linear relations given in eqs 11 and 12.

The results concerning the third criterion represent the most important part of the present study since the physical meaning of crystal field parameters becomes transparent. For reference, Table 3 presents the values of some relevant quantities across the series of Ln^{3+}, and the plots are shown in Figure 2a,b. The plot of Ln^{3+}(coordination number VI) radius has previously been interpreted as a tetrad variation.[20] However, plots of lattice parameter, a, and estimated Ln−Cl bond distance, R(Ln−Cl), can both be fitted by linear relations with very small uncertainties, (Figure 2a, in units of cm^{-10} m):

$$a = (10.953 \pm 0.006) - (226 \pm 6) \times 10^{-4}N \quad (13)$$

$$R(\text{Ln}-\text{Cl}) = (2.689 \pm 0.002) - (112 \pm 3) \times 10^{-4}N \quad (14)$$

The lattice constant is only changed by ca. 2% from Ln = Ce to Yb, and the bond length by ca. 5% in this range.

The values of the radial integrals r^k (in units of $(10^{-10}\ m)^k$) show a smooth contraction across the series (Figure 2b), fitted with confidence ($R^2 \sim 0.9995$) by:

$$r^2 = 0.274 \times \exp(-N/8.643) + 0.1282 \quad (15)$$

$$r^4 = 0.305 \times \exp(-N/5.828) + 0.0594 \quad (16)$$

$$r^6 = 0.555 \times \exp(-N/4.588) + 0.0632 \quad (17)$$

The r^4 and r^6 values for Yb^{3+} are 27 and 17% of the values for Ce^{3+}, respectively.

Figure 3 shows the scatter plot of the fourth-order crystal field parameters across the Ln^{3+} series and compares the data points with those calculated from a simple model. It is noted that $\exp[-Br(Ln^{3+})/r_{4f}(Ln^{3+})]$ is a semiquantitative measure of the distribution of the 4f radial wave function at the edge of the Ln^{3+} ion, where the ligand orbitals extend. In this function, $r(Ln^{3+})$ and $r_{4f}(Ln^{3+}) = \langle 4f|r^2|4f\rangle^{1/2}$ are the Ln^{3+}(VI) ionic radius, and a measure of the radius of the 4f orbitals in Ln^{3+}, respectively. This function has therefore been employed in the fitting of the crystal field parameter B_4 across the series:

$$B_4(Ln^{3+}) = \exp[A - Br(Ln^{3+})/r_{4f}(Ln^{3+})] \quad (18)$$

where $\exp(A) = [\exp(9.503)]\ cm^{-1}$, and $B = 1.094$ were taken as adjustable parameters. These are expected to depend on the host drastically and weakly, respectively. The fitting is satisfactory in Figure 3, showing that the value of B_4 is thus dominated by the nearest neighbor ligand. B_6 is much smaller and less important with much larger relative uncertainty across the lanthanide series. A fitting similar to eq 18 can be made, but the uncertainties of adjustable parameters turn out to be much bigger.

The final item for consideration concerns the parameter trends over various crystal hosts for a particular ion. A comparison can be made with some Cs_2NaLnF_6 systems although the available data are less extensive than for the chloride systems.[9,21] Considering the spin−orbit coupling constant, the available values of ζ_{4f}(F) for Ln = Eu, Tb, Er, Tm, Yb agree with the values of ζ_{4f}(Cl) within the uncertainties of determination. The comparison is given in Figure S5. Kawabe[20] has presented the variation of $[\zeta_{4f}]^{0.25}$ against Z using the experimental values

TABLE 3: Some Parameters of Trivalent Lanthanide Ions, with Reference to $Cs_2NaLnCl_6$[a]

Ln^{3+}	Ce	Pr	Nd	Pm	Sm	Eu	Gd	Tb	Dy	Ho	Er	Tm	Yb
N	1	2	3	4	5	6	7	8	9	10	11	12	13
$\langle r^2\rangle$ (10^{-20} m^2)	0.373	0.347	0.322	0.300	0.281	0.265	0.250	0.237	0.226	0.215	0.206	0.197	0.189
$\langle r^4\rangle$ (10^{-40} m^4)	0.316	0.279	0.241	0.211	0.187	0.168	0.151	0.138	0.126	0.115	0.106	0.099	0.092
$\langle r^6\rangle$ (10^{-60} m^6)	0.507	0.430	0.350	0.292	0.247	0.212	0.185	0.162	0.144	0.128	0.115	0.104	0.095
R(Ln-Cl) (10^{-10} m)	2.68	2.67	2.66	2.64	2.63	2.63	2.61	2.60	2.58	2.57	2.57	2.56	2.54
a (10^{-10} m)	10.945	10.911	10.889		10.834	10.809	10.791	10.760	10.743	10.727	10.704	10.686	10.656

[a] Radial integrals r^k (k = 2, 4, 6)[17] are in units of $(10^{-10}$ m$)^k$; calculated bond length, R(Ln−Cl)[18] and measured lattice constant, a,[19] are in units of 10^{-10} m.

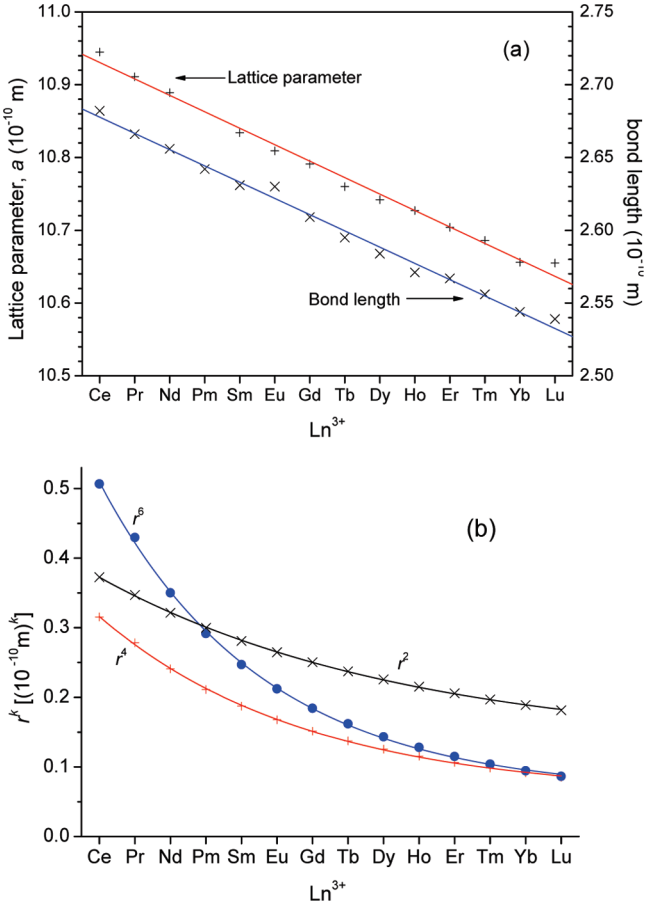

Figure 2. Variations across the Ln^{3+} series in $Cs_2NaLnCl_6$ of (a) lattice parameter, a, and estimated bond distance, R(Ln−Cl); (b) radial integrals r^2, r^4, and r^6 of Ln^{3+}.

for aquo ions from Carnall's work.[4] From the resulting linear plot the value of the 4f screening constant was evaluated to be 32.0. An analogous plot from the $Cs_2NaLnCl_6$ data, of $[\zeta_{4f}]^{0.25}$ against Z is presented in Figure S6 (N = 12; R = 0.9995). The derived equation is:

$$[\zeta_{4f}]^{0.25} = 0.193(Z - 31.9) = 0.193Z^* \qquad (19)$$

where Z^* is the effective nuclear charge, which gives a similar value (31.9) for the screening constant. The relationship between $\zeta_{4f}{}^{0.25}$ and F^2 from the present study is also linear (Figure S7).

Finally, in view of the nearest neighbor dominance, the comparison is given between the crystal field parameters for Cs_2NaLnX_6 (X = Cl, F) systems. The ratios of these parameters in Cs_2NaLnF_6 and $Cs_2NaLnCl_6$ are known for only Ln = Eu, Tb, Er, Tm, and Yb, and the uncertainties are very large. Within the uncertainties, those ratios can be considered as constant (Figure S8) and are deduced as:

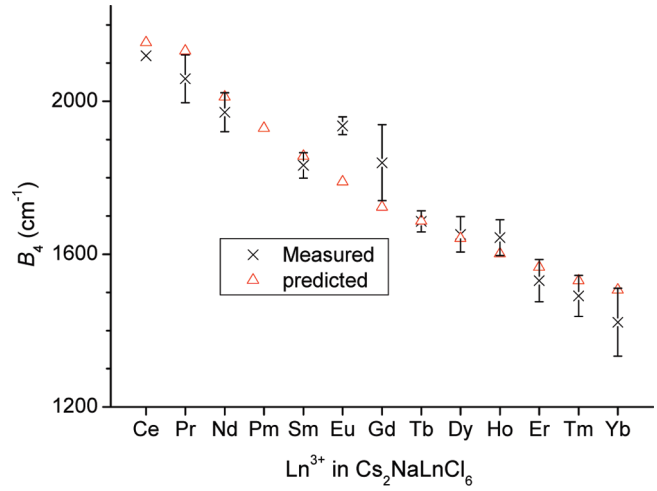

Figure 3. Measured crystal field parameters for Ln^{3+} in $Cs_2NaLnCl_6$ and predicted ones using eq 18.

$$B_4(\mathrm{F})/B_4(\mathrm{Cl}) = 1.77 \pm 0.27 \qquad (20)$$

$$B_6(\mathrm{F})/B_6(\mathrm{Cl}) = 1.81 \pm 0.78 \qquad (21)$$

With the use of these ratios, and equations 11 and 12 for the Ln^{3+} crystal field parameters in $Cs_2NaLnCl_6$, the corresponding equations for the fluoride hosts are deduced (in units of cm^{-1}):

$$B_4(\mathrm{F}) = (3852 \pm 52) - (100 \pm 6)N \qquad (22)$$

$$B_6(\mathrm{F}) = (517 \pm 45) - (23 \pm 5.0)N \qquad (23)$$

and the data are plotted in Figure 4.

Conclusions

Crystal field energy level fittings have been performed for lanthanide ions (Ln^{3+}) in the hexachloroelpasolite host lattice, $Cs_2NaLnCl_6$. This host has been chosen because the number of parameters required is the least possible for crystals, so that certain parameters are more unlikely to take on unrealistic values by absorbing errors resulting from false values of other parameters. Recent data from one- and two-photon spectroscopy have enlarged the energy level data sets for these systems. The crystal field analyses of these data sets yield smooth variations across the lanthanide series for the major parameters. The typical fitting accuracy for energy levels is ~20 cm^{-1} so that solid predictions can be made for the levels which are potentially

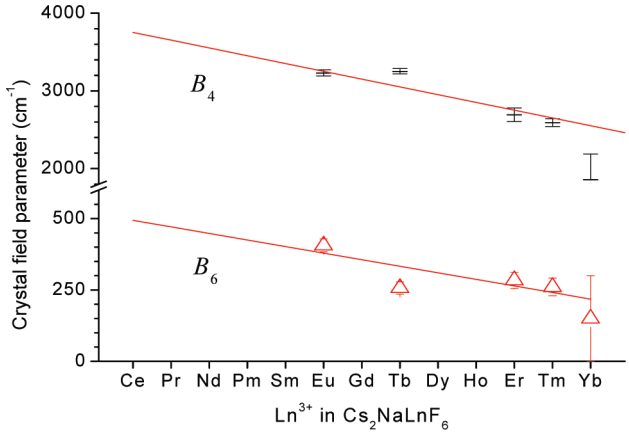

Figure 4. Measured and predicted crystal field parameters for Cs_2NaLnF_6 using eqs 22 and 23.

luminescent. An intuitive model has been presented to account for the variation of the fourth order crystal field parameter across the series. The nearest neighbor ligand plays a dominant role in this model and the results have also been extended to the hexafluoroelpasolite host lattice.

Acknowledgment. Financial support for this work under the Hong Kong University Grants Council Research Grant CityU 102308 is gratefully acknowledged.

Supporting Information Available: Supporting Information comprising the energy level structure of Pm^{3+} in $Cs_2NaPmCl_6$ (Table S1) and various plots of parameters and parameter value ratios against atomic number (Figures S1−S8) are available free of charge via the Internet at http://pubs.acs.org.

References and Notes

(1) Gruber, J. B.; Nijjar, A. S.; Sardar, D. K.; Yow, R. M.; Russell III, C. C.; Allik, T. H.; Zandi, B. *J. Appl. Phys.* **2005**, *97*, 063519. Gruber, J. B.; Sardar, D. K.; Yow, R. M.; Allik, T. H.; Zandi, B. *J. Appl. Phys.* **2004**, *96*, 3050–3056.

(2) Görller-Walrand, C.; Binnemans, K. *Handbook on the Physics and Chemistry of Rare Earths*; Gschneidner, Jr., K. A. Eyring, L. Eds.; Elsevier Science B.V.: 1996; Vol 23, pp 121−283.

(3) Williams, G. M.; Becker, P. C.; Conway, J. G.; Edelstein, N.; Boatner, L. A.; Abraham, M. M. *Phys. Rev. B* **1989**, *40*, 4132–4142. Guillot-Nöel, O.; Kahn-Harari, A.; Viana, B.; Vivien, D.; Antic-Fidancev, E.; Porcher, P. *J. Phys.: Condens. Matter* **1998**, *10*, 6491–6503.

(4) Jayasankar, C. K.; Richardson, F. S.; Reid, M. F. *J. Less-Common Met.* **1989**, *148*, 289–296. Carnall, W. T.; Goodman, G. L.; Rajnak, K.; Rana, R. S. *J. Chem. Phys.* **1989**, *90*, 3443–3457.

(5) Hölsä, J.; Lamminmäki, R. J. *J. Lumin.* **1996**, *69*, 311–317.

(6) Tanner, P. A. *Top. Curr. Chem.* **2004**, *241*, 167–278.

(7) Morrison, C. A.; Leavitt, R. P.; Wortman, D. E. *J. Chem. Phys.* **1980**, *73*, 2580–2598. Richardson, F. S.; Reid, M. F.; Dallara, J. J.; Smith, R. D. *J. Chem. Phys.* **1985**, *83*, 3813–3830. Reid, M. F.; Richardson, F. S. *J. Chem. Phys.* **1985**, *83*, 3831–3836. Tanner, P. A.; Kumar, V. V. R. K.; Jayasankar, C. K.; Reid, M. F. *J. Alloys Compd.* **1994**, *215*, 349–370.

(8) Chen, X.; Liu, G.; Margerie, J.; Reid, M. F. *J. Lumin.* **2008**, *128*, 421–427.

(9) Morrison, I. D.; Berry, A. J.; Denning, R. G. *Mol. Phys.* **1999**, *96*, 43–51. Thorne, J. R. G.; Jones, M.; McCaw, C. S.; Murdoch, K. M.; Denning, R. G.; Khaidukov, N. M. *J. Phys.: Condens. Matter* **1999**, *11*, 7851–7866. Thorne, J. R. G.; Zeng, Q.; Denning, R. G. *J. Phys.: Condens. Matter* **2001**, *13*, 7403–7419. Faucher, M. D.; Tanner, P. A. *J. Phys.: Condens. Matter* **2006**, *18*, 8503–8522. Zhou, X.; Mak, C. S. K.; Tanner, P. A.; Faucher, M. D. *Phys. Rev. B* **2006**, *73*, 075113. Zhou, X.; Tanner, P. A. *Chem. Phys. Lett.* **2005**, *413*, 284–288. Faucher, M. D.; Tanner, P. A. *Mol. Phys.* **2003**, *101*, 983–992. Tanner, P. A.; Mak, C. S. K.; Faucher, M. D. *J. Chem. Phys.* **2001**, *114*, 10860–10871. Burdick, G. W.; Richardson, F. S. *J. Alloys Compd.* **1997**, *250*, 293–296.

(10) Crosswhite, H. M.; Crosswhite, H. *J. Opt. Soc. Am. B* **1984**, *1*, 246–254.

(11) Tanner, P. A.; Duan, C. K.; Cheng, B. M. *Spectrosc. Lett.* in press.

(12) Tanner, P. A. *Chem. Phys. Lett.* **1988**, *145*, 134–138.

(13) Duan, C.-K.; Tanner, P. A. *J. Phys.: Condens. Matter* **2010**, *22*, 125503. 6 pp.

(14) Dieke, G. H. *Spectra and Energy Levels of Rare Earth Ions in Crystals*; Crosswhite, H. M. Crosswhite, H., Eds.; Intersci. Publ.: New York, 1968; pp 58−68.

(15) Hüfner, S. *Optical Spectra of Transparent Rare Earth Compounds*; Academic Press: New York, 1978; p 31.

(16) Faulkner, T. R.; Morley, J. P.; Richardson, F. S.; Schwartz, R. W. *Mol. Phys.* **1980**, *40*, 1481–1488.

(17) Reid, M. F.; van Pieterson, L.; Meijerink, A. *J. Alloys Compd.* **2002**, *344*, 240–245.

(18) Ordejon, B.; Seijo, L.; Barandiaran, Z. *J. Chem. Phys.* **2003**, *119*, 6143–6149.

(19) Meyer, G. *Progr. Solid St. Chem.* **1982**, *14*, 141–219.

(20) Kawabe, I. *Geochem. J.* **1992**, *26*, 309–335.

(21) Tanner, P. A.; Liu, Y.-L.; Edelstein, N.; Murdoch, K.; Khaidukov, N. M. *J. Phys.: Cond. Matter* **1997**, *9*, 7817–7836. Tanner, P. A.; Faucher, M. D. *Chem. Phys. Lett.* **2007**, *445*, 183–187. Zhou, X.-J.; Tanner, P. A.; Faucher, M. D. *J. Phys. Chem. C* **2007**, *111*, 683–687. Zhou, X.; Reid, M. F.; Faucher, M. D.; Tanner, P. A. *J. Phys. Chem. B* **2006**, *110*, 14939–14942.

JP1015214